A mass conservation approach for mapping glacier ice thickness

M. Morlighem,[1,2] E. Rignot,[1,3] H. Seroussi,[1,2] E. Larour,[1] H. Ben Dhia,[2] and D. Aubry[2]

Received 24 June 2011; revised 6 September 2011; accepted 8 September 2011; published 13 October 2011.

[1] The traditional method for interpolating ice thickness data from airborne radar sounding surveys onto regular grids is to employ geostatistical techniques such as kriging. While this approach provides continuous maps of ice thickness, it generates products that are not consistent with ice flow dynamics and are impractical for high resolution ice flow simulations. Here, we present a novel approach that combines sparse ice thickness data collected by airborne radar sounding profilers with high resolution swath mapping of ice velocity derived from satellite synthetic-aperture interferometry to obtain a high resolution map of ice thickness that conserves mass and minimizes the departure from observations. We apply this approach to the case of Nioghalvfjerdsfjorden (79North) Glacier, a major outlet glacier in northeast Greenland that has been relatively stable in recent decades. The results show that our mass conserving method removes the anomalies in mass flux divergence, yields interpolated data that are within about 5% of the original data, and produces thickness maps that are directly usable in high spatial-resolution, high-order ice flow models. We discuss the application of this method to the broad and detailed radar surveys of ice sheet and glacier thickness.
Citation: Morlighem, M., E. Rignot, H. Seroussi, E. Larour, H. Ben Dhia, and D. Aubry (2011), A mass conservation approach for mapping glacier ice thickness, *Geophys. Res. Lett.*, *38*, L19503, doi:10.1029/2011GL048659.

1. Introduction

[2] Important ice sheet characteristics such as ice thickness, surface elevation or surface velocity are most efficiently derived from airborne and satellite platforms carrying instruments operating at different spatial resolutions and deployed at different epochs. As a consequence, data sets are not always consistent with one another, and this complicates their combined use in numerical ice sheet models. For example in Greenland, surface ice velocity has been measured at a high spatial resolution (30–300 m) with satellite synthetic-aperture radar interferometry (InSAR), with low error margins (a few m/yr); whereas ice thickness has been derived from airborne radar sounding profilers, with tracks spaced by several to tens of kilometers, collected at different epochs, and interpolated onto a regular grid using geostatistical algorithms, e.g. kriging [*Deutsch and Joumel*, 1997]. The grid size selected for ice thickness mapping, typically 5 km in Greenland, is often much smaller than the actual average spacing between tracks [e.g., *Bamber et al.*, 2001], which means that the true spatial resolution of the data is much larger than the grid spacing.

[3] A recent study by *Seroussi et al.* [2011] revealed that combination of thickness data gridded by kriging with high resolution surface velocity data from InSAR generates major artifacts that severely limit the applicability of these data to high resolution ice sheet models. Namely, the ice flux divergence resulting from this combination exhibits large spatial deviations on grounded ice, exceeding several hundreds of m/yr, that are physically untenable, i.e., they cannot be explained in terms of temporal changes in thickness, surface mass balance or basal mass balance. If flow models are initialized with these data, the results diverge quickly from their initial state [*Rasmussen*, 1985]. Alternative solutions of assigning these errors to steady-state values of basal melting, have an uncertain but possibly significant impact on the reliability and relevance of the model results initialized in that manner.

[4] The underlying cause of these deviations in flux divergence is that the ice thickness data are used beyond their actual spatial resolution and their geostatistical interpolation onto a finer grid violates the conservation of mass. Kriging is a widely used technique of thickness interpolation in ice sheet surveying; while it may be appropriate to create background maps of bed topography that are continuous and regularly distributed, it leads to unrealistic behaviors in ice flow dynamics when used in high resolution ice sheet models because the small errors introduced in the uncontrolled interpolation of the data have a large impact on the ice flux divergence.

[5] Here, we propose a new approach, based on mass conservation, to infer ice thickness onto a high spatial-resolution mesh by combining sparse ice thickness data from radar sounding profilers with dense, high spatial-resolution ice velocity data collected by swath mapping satellites and ancillary data. The goal is to provide ice sheet models with robust and more reliable ice thickness maps, with fewer artifacts, and also estimate the spatial distribution of errors in ice thickness.

[6] The idea of using ice velocity to infer a spatially consistent map of ice thickness is not new. *Rasmussen* [1988] used this approach on Columbia Glacier using a finite difference scheme. *Fastook et al.* [1995] used the solution of polynomial of the fourth degree derived from the Shallow Ice Approximation (SIA) to calculate the ice thickness of Jakobshavn Isbræ, in West Greenland. *Warner and Budd* [2000] employed the SIA to calculate the ice thickness over the Antarctic Ice Sheet using mass flux conservation. *Farinotti et al.* [2009] employed a method, derived from the same principle, to determine the ice volume of Swiss alpine glaciers. All these studies, however, suffer from significant deviations from the original thickness data, i.e., by hundreds

[1]Jet Propulsion Laboratory, California Institute of Technology, Pasadena, California, USA.
[2]Laboratoire MSSMat, UMR 8579, CNRS, École Centrale Paris, Grande Voie des Vignes, Châtenay-Malabry, France.
[3]Department of Earth System Science, University of California, Irvine, California, USA.

0094-8276/11/2011GL048659

of meters in the case of *Fastook et al.* [1995] and *Warner and Budd* [2000], and an average 25% by *Farinotti et al.* [2009].

[7] In this study, we present a more advanced methodology to produce spatially consistent ice thickness data sets with much lower errors. After introducing the method and the optimization process, we discuss its application to a major Greenland outlet glacier, describe the results and conclude on the applicability of this approach to the broad, detailed surveys of glaciers and ice sheets.

2. Method

2.1. Balance Thickness

[8] If ice is treated as an incompressible material, mass conservation requires the velocity vector, $\mathbf{v}$, to be divergence free, $\nabla \cdot \mathbf{v} = 0$. Using the kinematics of the glacier bed and surface, this equation is vertically integrated using the Leibnitz integral rule to obtain the two-dimensional form of the mass conservation equation:

$$\frac{\partial H}{\partial t} + \nabla \cdot H\overline{\mathbf{v}} = \dot{M}_s - \dot{M}_b \tag{1}$$

where H is the ice thickness and $\overline{\mathbf{v}}(x,y) = (\overline{v}_x,\overline{v}_y)$ is the depth-averaged horizontal velocity, $\dot{M}_b$ is the basal melting rate (m/yr ice equivalent, positive when melting, negative when freezing), and $\dot{M}_s$ is the surface mass balance (m/yr ice equivalent, positive for accumulation, negative for ablation). This equation states that the ice flux divergence is balanced by the rate of thickness change and the net surface and basal mass balances.

[9] Let Ω be the two-dimensional ice domain and $\partial\Omega$ its boundary. We define the inflow and outflow boundaries as follows:

$$\begin{aligned} \Gamma_- &= \{\mathbf{x} \in \partial\Omega \quad \overline{\mathbf{v}}(\mathbf{x}) \cdot \mathbf{n}(\mathbf{x}) \leq 0\} \\ \Gamma_+ &= \{\mathbf{x} \in \partial\Omega \quad \overline{\mathbf{v}}(\mathbf{x}) \cdot \mathbf{n}(\mathbf{x}) > 0\} \end{aligned} \tag{2}$$

with $\mathbf{n}$ the outward-pointing unit normal vector. We also define $T \in \Omega$ as the flight tracks where data are collected within the model domain. The balance ice thickness is calculated by solving

$$\begin{cases} \nabla \cdot H\overline{\mathbf{v}} = \dot{a} & \text{in } \Omega \\ H = H_{obs} & \text{on } \Gamma_- \end{cases} \tag{3}$$

where $\dot{a} = \dot{M}_s - \dot{M}_b - \partial H/\partial t$, is the apparent mass balance following *Farinotti et al.* [2009] and H_{obs} is an observed thickness. This equation requires that ice thickness be constrained once and only once for each flow line. Constraining ice thickness at the inflow boundary is a simple way of achieving this condition. Note that even though we call this solution "balance thickness", it shall not be confused with the steady-state glacier thickness because it incorporates the rate of thickness change, $\partial H/\partial t$.

[10] Equation (3) is a steady hyperbolic partial differential equation of first order. Such equations are difficult to solve numerically [e.g., *Donea*, 1984]. Here we employ a streamline upwinding finite element method to solve it.

2.2. Multi-Parameter Optimization

[11] Solving for the balance thickness (equation (3)) requires precise knowledge of the apparent mass balance and ice velocity. These data sets are not always available, or include errors, which strongly affect the solution. For example, slight errors in the velocity data yield large errors in glacier thickness [*Rasmussen*, 1985]. To reduce these deviations, we optimize the apparent mass balance and depth-averaged velocity to minimize the misfit between observed and modeled ice thickness along the flight tracks, T. We define an objective function as

$$\mathcal{J} = \int_T \frac{1}{2}(H(\overline{\mathbf{v}},\dot{a}) - H_{obs})^2 dx \; + \; \gamma \int_\Omega \|\nabla H(\overline{\mathbf{v}},\dot{a})\|^2 d\Omega \tag{4}$$

The first term measures the mismatch between modeled and measured thickness and the second term is a regularizing constraint, which penalizes wiggles in ice thickness. The addition of regularization is essential to infer an ice thickness that is smooth enough yet close enough to the original data along flight tracks. γ is a parameter used to adjust the influence of the regularization in the objective function. A large value of γ will result in a smoother thickness map that deviates more significantly from the observations whereas a small value of γ will produce in a good fit with observations but with strong gradients in the proximity of flight tracks.

[12] Here, we use a projected gradient descent algorithm to minimize $\mathcal{J}$, while keeping the depth-averaged velocity, $\overline{\mathbf{v}}$, and the apparent mass balance, $\dot{a}$, within certain tolerances based on error margins. We stop the optimization when the cost function reaches a sufficiently low value, typically an average misfit of 30 m, which is comparable to the error in ice thickness measurements. A detailed description of the optimization is presented in the auxiliary material.[1]

[13] The tolerance interval for the apparent mass balance, $\dot{a}$, is defined here as the sum of errors in surface mass balance, basal melting rate and thickness change. For 79North Glacier, we estimate this error to be on the order of ±1 m/yr. The admissible space for $\dot{a}$ is therefore

$$\dot{a} \in \{\dot{a}_{obs} + \alpha, \quad \alpha \in [-1\ 1]\} \tag{5}$$

[14] The tolerance interval for ice velocity is more difficult to evaluate a priori. Even though nominal errors in ice velocity are around ±2 m/yr, ice thickness and velocity are usually not measured at the same time and surface velocity is not identical to depth-averaged velocity. In areas where ice is frozen to the bed, the depth-averaged velocity may be 15% lower. In that case, the approach discussed herein needs to be revised to include differences between surface and depth-averaged velocities through 3D modeling of ice sheet flow. Here, on 79North Glacier, differences between surface and depth-averaged velocities are at the 1% level [*Seroussi et al.*, 2011], so it is reasonable to use surface velocities. To allow enough flexibility in the optimization process, however, we need a tolerance on ice velocity that is larger than the nominal error. We obtain satisfactory results with a tolerance of ±50 m/yr, which is less than 5% of the

[1] Auxiliary materials are available in the HTML. doi:10.1029/2011GL048659.

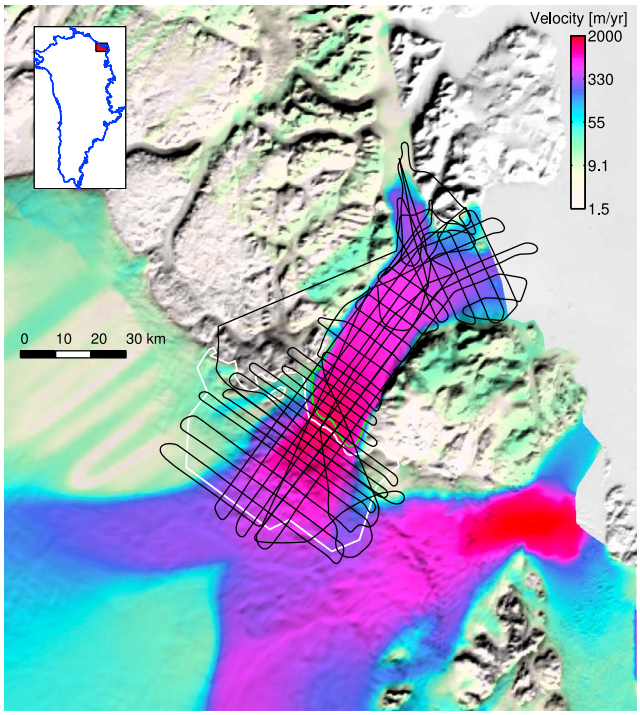

Figure 1. InSAR-derived surface velocity of 79North Glacier, in Greenland, color coded on a logarithmic scale and overlaid on a MODIS (Moderate-resolution Imaging Spectroradiometer) mosaic of Greenland. The flight tracks used in Reeh's thickness map are shown as black lines; the model domain is a white line; and the grounding line is the green line.

surface velocity of the main flow. The admissible space for $\overline{\mathbf{v}}$ becomes

$$\overline{v}_x \in \left\{\alpha_1 v_x^{obs} + \alpha_2, \quad \alpha_1 \in [0.95\ 1],\ \alpha_2 \in [-50\ 50]\right\} \tag{6}$$

$$\overline{v}_y \in \left\{\alpha_1 v_y^{obs} + \alpha_2, \quad \alpha_1 \in [0.95\ 1],\ \alpha_2 \in [-50\ 50]\right\} \tag{7}$$

[15] Given uncertainties in ice velocity, $\delta\overline{\mathbf{v}}$, and apparent mass balance, $\delta\dot{a}$, it is possible to estimate the maximum error in ice thickness, δH, as detailed in the supplementary material. Along a flow line, we show that the maximum error is given by

$$\delta H(x) = \frac{1}{\overline{v}(x)} \int_0^x \delta\dot{a} + |\nabla \cdot H\delta\overline{\mathbf{v}}|\, dx \tag{8}$$

where x is the curvilinear coordinate of the flow line starting from the inflow boundary. The error is therefore inversely proportional to the magnitude of the ice velocity. For a track spacing of 5 km and using values typical for 79North Glacier discussed next, the error in ice thickness is 10 m when ice velocity is about 1000 m/yr and 100 m when ice velocity is about 100 m/yr. This method is therefore most reliable in fast flowing areas.

3. Application to 79North Glacier

[16] In this section, we compare three methodologies to infer the ice thickness of 79North Glacier. The goal is to illustrate that the proposed optimization scheme achieves the best results. In experiment 1, we calculate the balance thickness by directly solving equation (3), with ice thickness only constrained on Γ_-; the flux divergence is imposed as equal to the apparent mass balance. In experiment 2, we impose ice thickness to be strictly equal to the measurements along the original tracks: the ice thickness is therefore constrained on both inflow boundary and flight tracks, T. Finally in experiment 3, we apply an optimization sequence that includes uncertainties velocity and apparent mass balance to best fit the observations without strongly constraining the thickness on T.

[17] The study area is the fast flowing portion of 79North Glacier, a large discharger of ice in north Greenland (Figure 1). This glacier has been extensively surveyed in the late 1990s, is not accelerating or changing in ice thickness at a significant level and hence provides a reliable, reference glaciological setting to test our algorithm. We use ice thickness from *Thomsen et al.* [1997] and *Christensen et al.* [2000] with a track spacing of 5 km on the upper part of the glacier, and 2.5 km near the grounding zone (Figure 1). A gridded thickness map at 1-km posting was generated by N. Reeh (unpublished data, 1998; Figure 2a) using block kriging, here referred to as Reeh's thickness map.

[18] Surface velocity is measured using ascending and descending tracks of the Earth Remote Sensing Satellite (ERS) 1 and 2 in year 1996 [*Rignot et al.*, 1997]. The ice stream velocity exceeds 1200 m/yr at the grounding line. The model domain is set by the geographic limits of Reeh's thickness map. This ensures that the input ice flux, which is an important control on the solution, is well constrained. Along parts of the inflow boundary where no measurement is available, we use Reeh's thickness map values to constrain the solution by default. We exclude floating parts of the glacier from the model domain because the basal melt rates on floating ice are not known well enough. Surface mass balance is from *Ettema et al.* [2009] and ranges from −120 cm/yr to −50 cm/yr averaged over the time period 1961–1996. Temporal changes in ice thickness are less than 1 m/yr [*Thomas et al.*, 2006] and are thus neglected. Basal melting on grounded ice is less than a few 10 cm per year and is neglected as well [*Fahnestock et al.*, 2001]. The apparent mass balance is therefore here taken as equal to the surface mass balance.

4. Results

[19] When Reeh's thickness map (Figure 2a) is combined with the observed surface velocities, we find a flux divergence on grounded ice that exceeds ±100 m/yr (Figure 2e), which is not physically acceptable. If an ice flow model is initiated in this manner, deep hollows and high bumps will rapidly appear, yielding a new glacier configuration significantly different from the original one.

[20] In experiment 1, we use an unstructured triangular mesh with a resolution of 400 m. The balance thickness shown in Figure 2b compares well with Reeh's thickness map, but deviates significantly from the measurements, by several hundreds of meters in some areas, which is not satisfactory.

[21] In experiment 2, we use the same spatial resolution but constrain the mesh to follow the flight tracks so that measurements can be imposed at their locations. Figure 2c

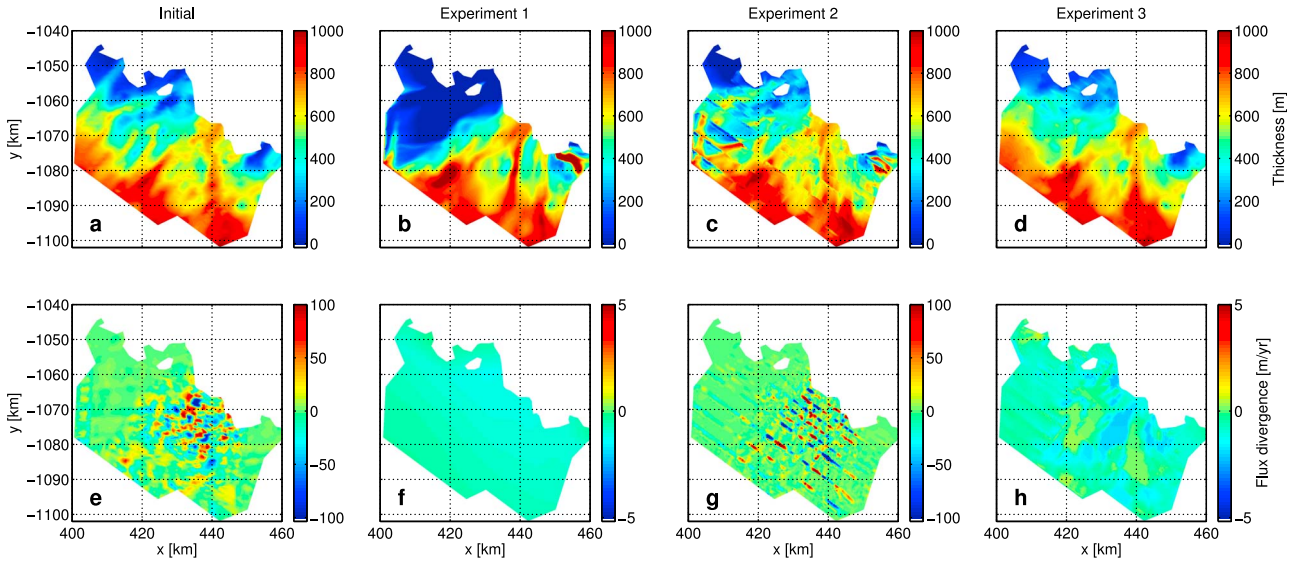

Figure 2. Thickness (m) of 79North Glacier, Greenland, from (a) N. Reeh, (b) experiment 1, (c) experiment 2, (d) experiment 3 (optimized calculation); and flux divergence (m/yr) combining InSAR velocities and the thickness map from (e) N. Reeh, (f) experiment 1 (apparent mass balance), (g) experiment 2, (h) experiment 3 (optimized calculation). Color bars associated with the flux divergence in Figures 2e and 2g have broader ranges to maintain visibility.

shows that the results fit the original data better but deviate rapidly from the measurements in between tracks and exhibit large jumps when crossing tracks, hence resulting in a noisy appearance of both ice thickness and flux divergence (Figure 2g). Indeed, the balance thickness hyperbolic equation requires the thickness to be constrained only once, it is incorrect to prescribe the thickness elsewhere. We therefore need to relax the constraints along the flight tracks by formulating an optimization problem.

[22] In experiment 3, which is the optimum algorithm we are proposing to use herein, we solve for equation (3) without additional constraint (same as experiment 1) but optimize the ice velocity and apparent mass balance within tolerance levels for the calculated thickness to best fit the thickness measurements along tracks. The resulting thickness map (Figure 2d) is close to Reeh's thickness, fits the original data well, and yields anomalies in flux divergence that are two orders of magnitude lower than the flux divergence associated to Reeh's thickness map (Figure 2h).

[23] Figure 3a compares Reeh's thickness data and the optimized balance thickness data in experiment 3 with observations. The balance thickness deviates by a factor 3 less from observations than Reeh's thickness map, i.e the error decreases from 80 to 30 m.

[24] Figure 3c shows error estimates for the balance thickness. The error is low along flight tracks and increases along the flow direction. Maximum errors are reached in between flight tracks, and the error increases when the track spacing increases. Errors are less than 30–50 m over the model domain. Along the sides of the domain, where ice thickness is weakly constrained by observations and ice velocity is low, errors exceed 120 m.

[25] Comparing our results with independent measurements of ice thickness from the Center for Remote Sensing of Ice Sheet (CReSIS) and Operation IceBridge (OIB) of years 1997, 1999, 2004 and 2010 in Figure 3b, we find an average difference of 43 m with the balance thickness and 73 m with Reeh's thickness map. This comparison therefore illustrates that our balance thickness is reliable and more accurate than the data obtained from kriging.

5. Discussion

[26] Our mass conservation approach provides seamless ice thickness data that conserves mass by combining ice velocity and ice thickness data in an optimum fashion, i.e., with no artifacts in ice flux divergence. Kriging provides interpolated data that do not deviate largely from the measurements but that do not conserve mass between flight tracks. Our analysis of errors shows that the maximum error in ice thickness is inversely proportional to ice velocity. Our method therefore yields optimal results in fast flowing regions, which is also a region of most relevance to ice sheet flow models because fast flowing regions have a major impact on ice sheet mass balance. The approach is less reliable in slow moving areas, where our assumption of no difference between surface velocity and depth-averaged velocity is less applicable, but this is also a part of the ice sheet where anomalies in ice flux divergence are quite small (Figure 2e). The algorithm is therefore optimum where it matters most.

[27] As demonstrated in this study, the solution to equation (3) is very sensitive to small errors in the input data. The hyperbolic nature of this equation leads to unstable solutions, especially in slow moving areas. In order to use this method most effectively it is therefore essential to have a good understanding of the error budget of the variables in equation (3).

[28] Our error analysis provides useful guidelines for ice thickness mapping in areas where ice velocity data are available. Errors in balance thickness are proportional to the distance to the closest track, so dense tracks are required, as expected. The preferable configuration of tracks is one that crosses as many flow lines as possible in order to constrain the

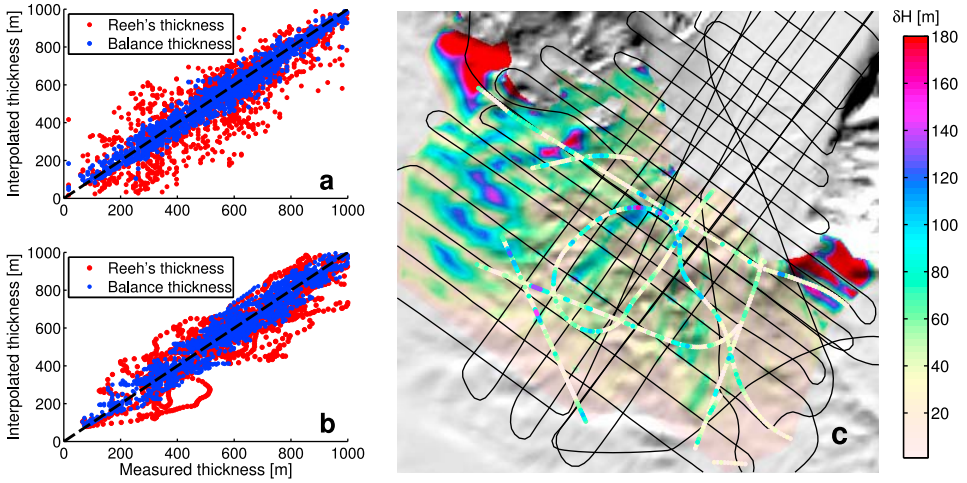

Figure 3. (a) Reeh's thickness (red dots) and balance thickness (blue dots) vs measurements used to generate both maps. (b) Reeh's thickness (red dots) and balance thickness (blue dots) vs CReSIS/OIB independent measurements. (c) Estimated maximum error in balance thickness (m) overlaid by the error between balance thickness and CReSIS/OIB measurements along flight lines. Flight tracks used in Reeh's thickness map are shown as black lines.

flux of the largest possible region of the domain. In contrast, a flight track that follows a flow line cannot constrain the flux of other flow lines. We therefore recommend glacier surveys preferably with tracks perpendicular to the flow direction; tracks along the flow direction will remain useful for flow line modeling and for estimating cross-track errors, but not so much for dense interpolation of ice thickness data using a mass conservation approach.

[29] Our method is applicable to other glaciers for which surface velocity and surface mass balance are known. On 79North Glacier, the apparent mass balance is small and almost negligible. On a fast changing glacier like Jakobshavn Isbræ, the rates of thickness change are large (15–30 m/yr), the apparent mass balance is not negligible and measurements of $\partial H/\partial t$ are needed to reduce uncertainties in calculated balance thickness.

[30] On floating ice shelves, our method is difficult to apply because the high rates of basal melting from the ocean are not well known, yet the anomalies in ice flux divergence are also much smaller [*Rignot and Steffen*, 2008]. More important, ice-shelf thickness may be more effectively deduced from digital maps of surface elevation assuming that ice is in hydrostatic equilibrium, so the mass conservation approach is less critical to obtaining reliable gridded ice thickness maps.

6. Conclusions

[31] We present an alternative solution to the traditional mapping of ice thickness with kriging, which has shown serious limitations for ice sheet modeling applications. Our technique is applicable to any glaciated terrain for which information on apparent mass balance data is available, and most important for those for which dense measurements of ice velocity exist. Our method is most effective in fast flowing regions, where ice sheet models need it most. It provides data sets that can readily be used in ice sheet models, fit the observations well and generate no anomalies in flux divergence, thereby increasing confidence in model results. In one example, our approach reduces errors in ice thickness by a factor 2, to less than 40 m, or 5% of the total thickness. The algorithm is available in the Ice Sheet System Model (http://issm.jpl.nasa.gov) [*Morlighem et al.*, 2010].

[32] **Acknowledgments.** This work was performed at the Jet Propulsion Laboratory, California Institute of Technology, at the Department of Earth System Science, University of California Irvine, and at Laboratoire MSSMat, École Centrale Paris, under a contract with the NASA Cryospheric Sciences Program. The authors thank two anonymous reviewers for helpful and insightful comments. We would also like to acknowledge the use of data and/or data products from CReSIS and OIB, which greatly helped to evaluate our method.

[33] The Editor thanks Ben Smith and an anonymous reviewer for their assistance in evaluating this paper.

References

Bamber, J., R. Layberry, and S. Gogineni (2001), A new ice thickness and bed data set for the Greenland ice sheet: 1. Measurement, data reduction, and errors, *J. Geophys. Res.*, *106*(D24), 33,773–33,780.

Christensen, E. L., N. Reeh, R. Forsberg, J. H. Jørgensen, N. Skou, and K. Woelders (2000), A low-cost glacier-mapping system, *J. Glaciol.*, *46*(154), 531–537.

Deutsch, C., and A. Joumel (1997), *GSLIB. Geostatistical Software Library and User's Guide*, *2nd ed.*, Oxford Univ. Press, New York.

Donea, J. (1984), Recent advances in computational methods for steady and transient transport problems, *Nucl. Eng. Design*, *80*(2), 141–162, doi:10.1016/0029-5493(84)90163-8.

Ettema, J., M. R. van den Broeke, E. van Meijgaard, W. J. van de Berg, J. L. Bamber, J. E. Box, and R. C. Bales (2009), Higher surface mass balance of the Greenland ice sheet revealed by high-resolution climate modeling, *Geophys. Res. Lett.*, *36*, L12501, doi:10.1029/2009GL038110.

Fahnestock, M., W. Abdalati, I. Joughin, J. Brozena, and P. Gogineni (2001), High geothermal heat row, basal melt, and the origin of rapid ice how in central Greenland, *Science*, *294*(5550), 2338–2342.

Farinotti, D., M. Huss, A. Bauder, M. Funk, and M. Truffer (2009), A method to estimate the ice volume and ice-thickness distribution of alpine glaciers, *J. Glaciol.*, *55*(191), 422–430.

Fastook, J., H. Brecher, and T. Hughes (1995), Derived bedrock elevations, strain rates and stresses from measured surface elevations and velocities: Jakobshavns Isbrae, Greenland, *J. Glaciol.*, *41*(137), 161–173.

Morlighem, M., E. Rignot, H. Seroussi, E. Larour, H. Ben Dhia, and D. Aubry (2010), Spatial patterns of basal drag inferred using control methods from a full-Stokes and simpler models for Pine Island Glacier, West Antarctica, *Geophys. Res. Lett.*, *37*, L14502, doi:10.1029/2010GL043853.

Rasmussen, L. (1985), Adjusting two-dimensional velocity data to obey continuity, *J. Glaciol.*, *31*(108), 115–119.

Rasmussen, L. (1988), Bed topography and mass-balance distribution of Columbia Glacier, Alaska, USA, determined from dequential serial-photography, *J. Glaciol.*, *34*(117), 208–216.

Rignot, E., and K. Steffen (2008), Channelized bottom melting and stability of floating ice shelves, *Geophys. Res. Lett.*, *35*, L02503, doi:10.1029/2007GL031765.

Rignot, E., S. Gogineni, W. Krabill, and S. Ekholm (1997), North and northeast Greenland ice discharge from satellite radar interferometry, *Science*, *276*(5314), 934–937.

Seroussi, H., M. Morlighem, E. Rignot, E. Larour, D. Aubry, H. Ben Dhia, and S. S. Kristensen (2011), Ice flux divergence anomalies on 79north Glacier, Greenland, *Geophys. Res. Lett.*, *38*, L09501, doi:10.1029/2011GL047338.

Thomas, R., E. Frederick, W. Krabill, S. Manizade, and C. Martin (2006), Progressive increase in ice loss from Greenland, *Geophys. Res. Lett.*, *33*, L10503, doi:10.1029/2006GL026075.

Thomsen, H., N. Reeh, O. Olesen, C. Boggild, W. Starzer, A. Weidick, and A. Higgins (1997), The Nioghalvfjerdsfjorden glacier project, north-east Greenland: A study of ice sheet response to climatic change, *Geol. Surv. Greenland Bull.*, *179*, 95–103.

Warner, R., and W. Budd (2000), Derivation of ice thickness and bedrock topography in data-gap regions over Antarctica, *Ann. Glaciol.*, *31*, 191–197.

D. Aubry and H. Ben Dhia, Laboratoire MSSMat, UMR 8579, CNRS, École Centrale Paris, Grande Voie des Vignes, F-92295 Châtenay-Malabry CEDEX, France.

E. Larour, M. Morlighem, and H. Seroussi, Jet Propulsion Laboratory, California Institute of Technology, 4800 Oak Grove Dr., MS 300-227, Pasadena, CA 91109-8099, USA. (Mathieu.Morlighem@jpl.nasa.gov)

E. Rignot, Department of Earth System Science, University of California, Croul Hall, Irvine, CA 92697-3100, USA.